Uptake of HCl(g) and HBr(g) on Ethylene Glycol Surfaces as a Function of Relative Humidity and Temperature

Y. Q. Li, H. Z. Zhang, and P. Davidovits*

Chemistry Department, Merkert Chemistry Center, Boston College, Chestnut Hill, Massachusetts 02467

J. T. Jayne, C. E. Kolb, and D. R. Worsnop

Center for Aerosol and Cloud Chemistry, Aerodyne Research Inc., 45 Manning Road, Billerica, Massachusetts 01821

Received: July 24, 2001; In Final Form: November 5, 2001

Organic compounds are a significant component of tropospheric aerosols. In the present experiments, ethylene glycol was selected as a surrogate hydrophilic organic compound for a study of surface properties of organic liquid−aqueous solutions. The mass accommodation coefficient of gas-phase HCl and HBr on ethylene glycol−water surfaces has been measured as a function of water mole fraction (0−1) and temperature. The gas uptake studies were performed under liquid−vapor equilibrium conditions using a droplet train flow reactor. The mass accommodation coefficient (α) for HCl on pure ethylene glycol increases from about 0.40 ± 0.06 at 303 K to 0.79 ± 0.12 at 258 K. Such negative temperature dependence for α has been observed in studies of gas uptake by aqueous surfaces. The HBr mass accommodation coefficient on ethylene glycol is near unity independent of temperature in the range studied. The mass accommodation coefficient on the ethylene glycol−water solution is well represented by $\alpha = \alpha_{H_2O}X(s)_{H_2O} + \alpha_{EG}(1 - X(s)_{H_2O})$, where $X(s)_{H_2O}$ is the water fractional surface coverage obtained via the surface tension of the solution and the subscripted α's are the mass accommodation coefficients on pure water and pure ethylene glycol. The D−H isotope exchange probability of DCl on the gas−liquid interface of ethylene glycol was also studied and was measured to be 1, implying that the thermal accommodation coefficient is also 1.

Introduction

Over the past few years increasing attention has been focused on tropospheric aerosols because of their health effects and their influence on climate and atmospheric chemistry. A recent study, for example, has shown that aerosols, specifically cloud condensation nuclei, originating from sources such as power plants, shut off precipitation from clouds.[1] The potential atmospheric chemical effects of aerosols have been stressed by several studies (see, for example, refs 2−4).

Tropospheric aerosols were initially envisioned as consisting mainly of inorganic salts and minerals. More recent field studies have shown that their composition is far more complex. An important recent development in atmospheric chemistry is the recognition that organic aerosols are abundant in many regions of the troposphere and represent a significant mass fraction in tropospheric aerosols. Over the continental USA the percentage of organic compounds in these aerosols is in the range of 20−50% and is often higher than 50% in polluted urban areas (see, for example, refs 5−11).

Organic aerosols, as do other aerosols, affect the atmospheric radiative budget (see, for example, Faccini et al.[12]). Exploratory studies indicate that organic aerosols are likely to play an important role in the chemistry of the atmosphere.[13] Further, secondary organic hydrophilic aerosols can serve as cloud condensation nuclei, often as effectively as inorganic sulfate aerosols.[7,9,14,15]

During the past decade, considerable phenomenological information has been gathered about organic aerosols. They are categorized as either primary or secondary originating from both anthropogenic and biogenic sources. Primary organic matter is emitted directly in particle phase. Initially, primary organics are hydrophobic, but subsequent oxidative reactions may render them more hydrophilic.[14] Secondary aerosols are formed via sulfur, nitrogen, and organic gas-phase species injected into the atmosphere.[16−18] Some of these gases are partially oxidized either in combustion or during their residence in the atmosphere, forming low vapor pressure products (see, for example, laboratory experiments of Odum et al.[19,20]). The oxidized species then either form new particles or condense on existing aerosols. The secondary organic fraction is composed of lower molecular weight, polar, hydrophilic species such as carboxylic[21] and dicarboxylic acids.[8,9,22] However, much about the formation, evolution, and important interactions of organic aerosols remains unknown.[23,24]

The composition of organic aerosols is highly complex, containing hundreds of compounds with a large fraction still unidentified.[14,24,25] To obtain basic information about the atmospheric behavior of organics, in the face of such complexity, one must select for study surrogate compounds representing classes of organics in aerosols. In this our first study, we have measured the uptake of gas-phase HCl and HBr on a pure ethylene glycol surface as a function of temperature ($T = 258$−303 K for HCl, 262−293 K for HBr) and on ethylene glycol−water surfaces as a function of water mole fraction (0−1) and temperature (at 273 and 293 K for HCl, at 273 and 283 K for HBr). The uptake studies were performed under liquid−vapor equilibrium conditions using a droplet train flow reactor. The uptake of DCl on an ethylene glycol surface was also measured.

10.1021/jp012861f CCC: $22.00
Published on Web 01/29/2002

While ethylene glycol is not an important component of the atmosphere, it is a convenient surrogate for hydrophilic organic compounds. HCl and HBr uptake studies probe the nature of hydrophilic organic surfaces as a function of relative humidity. The uptake studies yielded two fundamental parameters that influence gas−liquid interactions: the mass accommodation coefficient (α) and the thermal accommodation coefficient (S). The mass accommodation coefficient is the probability that a gaseous molecule striking a liquid surface enters into the bulk liquid phase. The thermal accommodation coefficient is the fraction of collisions that result in the kinetic and vibrational/rotational energies of the impinging gas molecule equilibrating with the mean energy of the liquid surface molecules.

Gas−Liquid Interactions

In the droplet train apparatus, discussed in the following section, a gas-phase species interacts with liquid droplets and the disappearance of that species from the gas phase is monitored. A phenomenological description of the entry of gases into liquids is straightforward. First, the gas-phase molecule is transported to the liquid surface, usually by gas-phase diffusion. The initial entry of the species into the liquid is governed by the mass accommodation coefficient, α, which is the probability that an atom or molecule striking a liquid surface enters into the bulk liquid phase.

In the absence of surface reactions, the mass accommodation coefficient determines the maximum flux, J, of gas into a liquid, which is given by

$$J = \frac{n_g \bar{c} \alpha}{4} \tag{1}$$

Here n_g is the density of the gas molecules of interest and $\bar{c}$ is their average thermal speed. If reactions occur at the gas−liquid interface, then the flux of species disappearing from the gas phase may exceed that given by eq 1. Of course, the flux cannot exceed the collision rate $(n_g\bar{c})/4$.

In a laboratory experiment, gas uptake by the liquid is usually limited by gas-phase diffusion and often by solubility constraints as the species in the liquid approaches Henry's law saturation. In the latter process, some of the molecules that enter the liquid evaporate back into gas phase due to the limited solubility of the species. As expected, this effect increases with gas−liquid interaction time. At equilibrium, the liquid is saturated and the flux of molecules into the liquid is equal to the rate of desorption of these molecules out of the liquid. The net uptake is then zero. Chemical reactions of the solvated species in the bulk liquid can provide a sink for the species, reducing the effect of saturation, and this increases the species uptake from the gas phase. In experiments subject to these effects, the measured flux ($\boldsymbol{J}$) into a surface is expressed in terms of a measured uptake coefficient, γ_{meas}, as

$$J = \frac{n_g \bar{c} \boldsymbol{\gamma_{meas}}}{4} \tag{2}$$

The effect of solubility on gas uptake has been described analytically in our previous publications (see, for example, Shi et al.[26]). In the present HCl(g) and HBr(g) studies, as will be shown, solubility does not limit gas uptake on the scale of gas−liquid experimental interaction times (2.5−17 ms). Therefore, only the effect of gas-phase diffusion on the uptake needs to be taken into account.

To a good approximation the effect of gas-phase diffusion and mass accommodation on the uptake can be decoupled, and γ_{meas} can be expressed as[26,27]

$$\frac{1}{\gamma_{meas}} = \frac{1}{\Gamma_{diff}} + \frac{1}{\alpha} \tag{3}$$

Here Γ_{diff} represents the effect on uptake when gas-phase diffusive transport does not fully keep up with the rate of trace gas uptake into the liquid.

Gas-phase diffusive transport of a trace gas to a train of moving droplets does not lend itself to a straightforward analytical solution; analytical solutions are not available even for a single stationary droplet over the full range of relevant Knudsen numbers (Kn). However, an empirical formulation of diffusive transport to a stationary droplet developed by Fuchs and Sutugin[28] has been shown to be in good agreement with measurements.[29,30]

Using the Fuchs−Sutugin formulation, Γ_{diff} is expressed as[31]

$$\frac{1}{\Gamma_{diff}} = \frac{0.75 + 0.283Kn}{Kn(1 + Kn)} \tag{4}$$

Here, $Kn = 2\lambda/d_f$; $\lambda = 3D_g/\bar{c}$ is the gas-phase mean free path, d_f is the effective diameter of droplets for the diffusive process, and D_g is the diffusion coefficient of the trace gas in the background gas obtained as in ref 32.

Extensive experiments have demonstrated that, with a simple modification, the Fuchs−Sutugin formulation provides a good representation of diffusive transport to a train of closely spaced moving droplets. In the modified expression, $\boldsymbol{d_f}$ in eq 4, is made equal to $2d_o$, where the d_o is the diameter of the droplet-forming orifice.[26,27]

Mass accommodation can be viewed as a two-step process involving surface adsorption followed by a competition between desorption and solvation.[26,33] First, the gas molecule strikes the surface and is thermally accommodated. The adsorption rate constant is $k_{ads} = S\bar{c}/4$. This adsorbed surface species then either enters the liquid (k_{sol}) or desorbs (k_{des}) from the surface. Solving the rate equations for the process leads to[26]

$$\frac{\alpha}{\boldsymbol{S} - \boldsymbol{\alpha}} = \frac{\boldsymbol{k_{sol}}}{\boldsymbol{k_{des}}} \tag{5}$$

In the uptake experiments with the isotope DCl, interfacial D−H isotope exchange opens a new channel for the disappearance of the gas-phase species. In this case, two factors are responsible for the measured disappearance of the gas-phase species:[34] (1) isotope exchange at the gas−liquid interface, with probability p_{ex}, and (2) uptake into the bulk liquid of the gas-phase species that has not undergone isotope exchange, with a probability of $\alpha(1 - p_{ex})$.

The unexchanged molecules entering the bulk are subject to isotope exchange within the liquid, but this does not add to the measured uptake of the species since this uptake is taken into account by the mass accommodation coefficient. Therefore, γ_{meas} is given by[34]

$$\frac{1}{\gamma_{meas}} = \frac{1}{\Gamma_{diff}} + \frac{1}{\alpha(1 - p_{ex}) + p_{ex}} \tag{6}$$

Experimental Description

In the droplet train apparatus shown in Figure 1,[32,26] a fast-moving monodisperse, spatially collimated train of droplets is produced by forcing a liquid through a vibrating orifice located in a separate chamber. In this experiment the liquid is an ethylene glycol−water solution with the water mole fraction

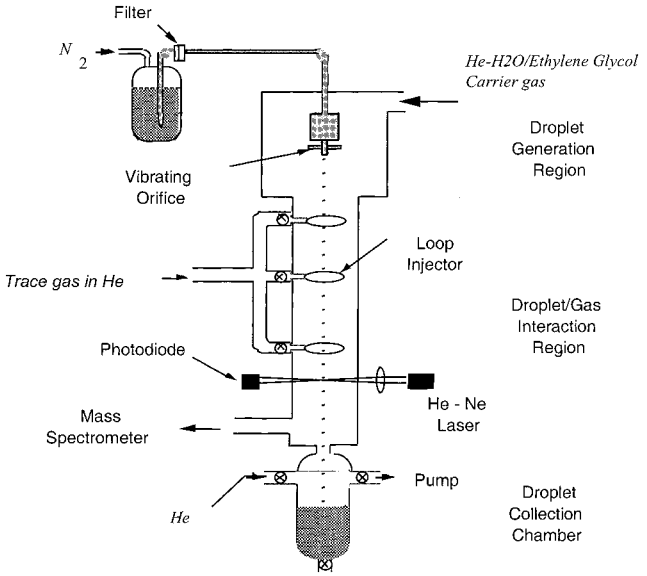

Figure 1. Schematic of droplet train flow reactor apparatus. Description is found in the text.

varied from 0 to 1 depending on the experimental run. Ethylene glycol at 99% stated purity was obtained from Sigma-Aldrich Inc., and the water was deionized and filtered with a Millipore system. The speed of the liquid droplets is in the range 1500−3000 cm s^{-1} determined by the pressure of the gas that forces the liquid through the orifice, and the orifice diameter. The droplet train is passed through a ∼30 cm long, 1.4 cm diameter, longitudinal low pressure (2−19 Torr) flow reactor that contains the trace gas species, in this case HCl, DCl, or HBr, at a density between 2×10^{13} and 3×10^{14} cm^{-3}.

The trace gas is entrained in a flowing mixture of an inert gas (usually helium) and ethylene glycol−water vapor mixture at equilibrium pressure with the liquid ethylene glycol−water droplets. The trace gas is introduced through one of three loop injectors located along the flow tube. By selecting the gas inlet port and the droplet velocity, the gas−droplet interaction time can be varied between about 2.5 and 17 ms.

Experimental results obtained in the temperature range from 298 to 363 K show that the equilibrium vapor pressure for an ethylene glycol−water solution follows Raoult's law to within about 6%.[35−37] We have assumed that Raoult's law continues to apply over the temperature range of our experiments (273−293 K), and the equilibrium ethylene glycol−water vapor mixture was prepared accordingly. Two separate flows containing a known fraction of water and ethylene glycol vapors are produced by bubbling helium gas through the two liquids, in separate temperature-controlled bubblers. The two flows are introduced into the droplet generation region at the entrance of the flow tube reactor. The required equilibrium ethylene glycol−water vapor mixture is obtained by adjusting the two helium carrier gas flows, to set the appropriate total pressure in the flow tube.

Orifices of two diameters 30 and 70 μm were used in these studies. Depending on the frequency of orifice vibration and the liquid flow rate, these orifices generate droplets in the ranges of 70−130 μm and 150−300 μm in diameter, respectively. Droplet formation frequencies range from 8 to 45 kHz. The uniformity of the droplets and the droplet velocity along the flow tube are monitored by passing cylindrically focused He−Ne laser beams through the droplet train at three heights along the flow tube.[27] The droplet velocity along the flow tube is measured to be constant to within 3%. Note that these droplets are large enough that their curvature has a negligible effect on the equilibrium vapor pressure.

The diameter, and hence the surface area, of the droplets passing through the flow tube is changed in a stepwise fashion by changing the driving frequency applied to the piezo ceramic in contact with the droplet-forming orifice. The density of the trace gas is monitored with a quadrupole mass spectrometer. The uptake coefficient (γ_{meas}) as defined by eq 2 is calculated from the measured change (Δn_g) in trace gas signal via[32]

$$\gamma_{meas} = \frac{4F_g}{\bar{c}\Delta A} \ln \frac{n_g}{n_g'} \qquad (7)$$

Here F_g is the carrier gas volume rate of flow (∼80−600 cm^3 s^{-1}) through the system, $\Delta A = A_1 - A_2$ is the change in the total droplet surface area in contact with the trace gas, and n_g and n_g' are the trace gas densities at the outlet of the flow tube after exposure to droplets of area A_2 and A_1, respectively ($n_g = n_g' + \Delta n_g$).

An important aspect of the experimental technique is the careful control of all the conditions within the apparatus, especially the ethylene glycol−water vapor pressure in the droplet generation chamber and in the flow tube. The temperature of the droplets is determined by the partial pressure of the equilibrium vapor in this region.[32] Experiments with pure ethylene glycol were performed between 258 and 303 K, where the equilibrium ethylene glycol vapor pressure varies from 0.005 Torr to 0.21 Torr. Detailed measurements with the ethylene glycol−water surfaces were performed at two temperatures: for HCl at 273 and 293 K and for HBr at 273 and 283 K. In these studies, depending on the droplet composition, the water vapor pressure ranged from 0 to 4.6 Torr at 273 K, from 0 to 9.2 Torr at 283 K, and from 0 to 17.5 Torr at 293 K. The ethylene glycol vapor pressure ranged from 0 to 0.019 Torr at 273 K, from 0 to 0.04 Torr at 283 K, and from 0 to 0.1 Torr at 293 K.

In the experiments conducted at lower temperatures, delivery lines were cooled to reduce the amount of evaporative cooling necessary to reach the desired final droplet temperature. Inert carrier gas (typically helium) was added to the vapor at a partial pressure of about 2−6 Torr. Overall pressure balance in the flow tube was checked by monitoring simultaneously both the trace species studied and the concentration of an inert reference gas, in this case Kr and Xe. These gases are effectively insoluble in the liquid droplets and have diffusion properties similar to those of HCl(g) and HBr(g), respectively. Any change in the reference gas concentration with droplet switching determines the "zero" of the system and was subtracted from observed changes in trace gas concentration. In the present experiments this correction was always less than 5%.

Results and Analysis

In Figure 2 we show a plot of $\ln(n_g/n_g')$ for HCl and HBr as a function of $\bar{c}\Delta A/4F_g$ at 273 K with the 70 μm diameter droplet-forming orifice. Here $\bar{c}\Delta A/4F_g$ was varied by changing the gas flow rate and the droplet surface area (ΔA). Each point is the average of at least 10 area change cycles, and the error bars represent one standard deviation from the mean in the experimental $\Delta n/n$ value. As is evident in eq 7, the slope of the plots in Figure 2 yields the value of γ_{meas}, in this case with a precision of ∼2%. These data yield $\gamma_{meas} = 0.50 \pm 0.01$ and 0.63 ± 0.02 for HCl and HBr, respectively. Similar plots were obtained for a wide range of experimental parameters, for which the uptake fraction, $\Delta n/n$, varied from 5% to 50%.

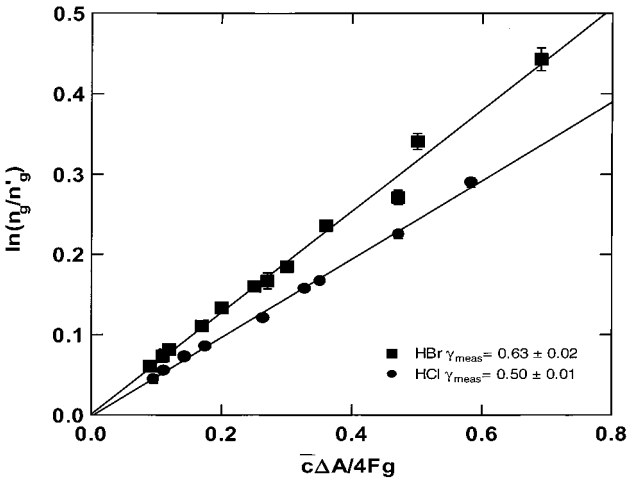

Figure 2. Experimental data showing plots of $\ln(n_g/n_g')$ as a function of $\bar{c}\Delta A/4F_g$ for HCl (circles) and HBr (squares) at droplet temperature $T_d = 273$ K with the 70 μm diameter droplet-forming orifice. Solid lines are the least-squares fit to the data. The slope of the lines is γ_{meas}. Terms are defined in the text.

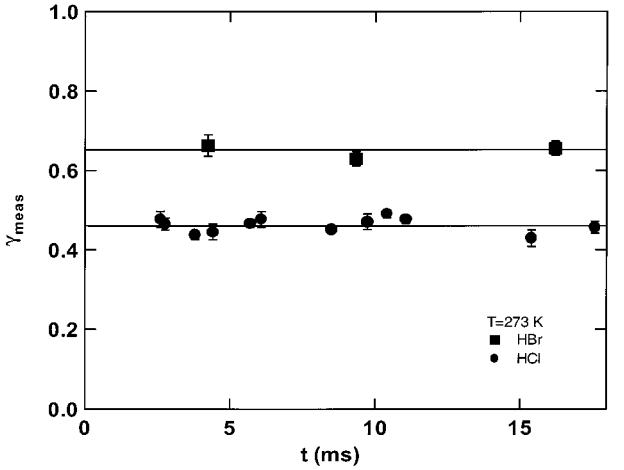

Figure 3. Uptake coefficient γ_{meas} for HCl (circles) and HBr (squares) as a function of gas−liquid contact time at droplet temperature $T_d = 273$ K. Solid lines are best straight-line fits to the data.

In Figure 3, γ_{meas} at $T = 273$ K is plotted as a function of gas−droplet contact time for HCl and HBr. The solid line is the best linear fit to the data. As is evident, over our experimental time scales and within the precision of the data, the trace gas uptake is not dependent on the gas−droplet interaction time. The measured time dependence of the uptake coefficients is similar at the other temperatures studied. Therefore, as was stated earlier, in these studies solubility does not limit gas uptake.

Uptake is measured at the lowest background pressure consistent with the required equilibrium vapor pressure of droplets and the necessary inert carrier gas flow. To study the effect of gas-phase diffusive transport, the gas uptake was then also measured as a function of increasing inert gas background pressure and with different inert gases, significantly changing the Knudsen number. As noted, droplet forming orifices of two diameters were used (70 and 30 μm), generating droplet diameters ranging from 70 to 300 μm. The uptake coefficients γ_{meas} for HCl at 273 K and for DCl and HBr on pure ethylene glycol droplets, as a function of *Kn*, are shown in Figure 4. For DCl and HBr, γ_{meas} is independent of temperature, in the studied range 267−293 K. The solid lines are best fits to the data via eq 3 for HCl and HBr and eq 6 for DCl with Γ_{diff} given by

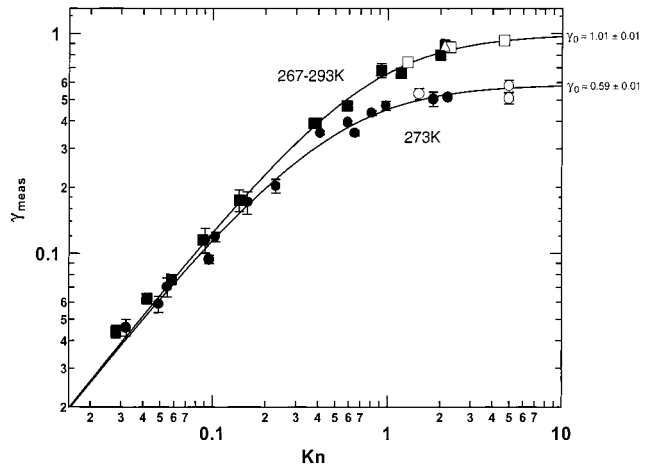

Figure 4. Uptake coefficient γ_{meas} as a function of Knudsen number (*Kn*) for HCl (circles) at 273 K and for DCl (triangles) and HBr (squares) in the temperature range 267−293 K. Open symbols were obtained with the 30 μm orifice, filled symbols with the 70 μm orifice. The solid lines are best fits to data via eq 3 for HCl and HBr and eq 6 for DCl with Γ_{diff} given by eq 4. The asymptote at large *Kn*, designated as γ_0, is the uptake coefficient in the limit of "zero pressure", i.e., in the absence of gas-phase diffusion limitation.

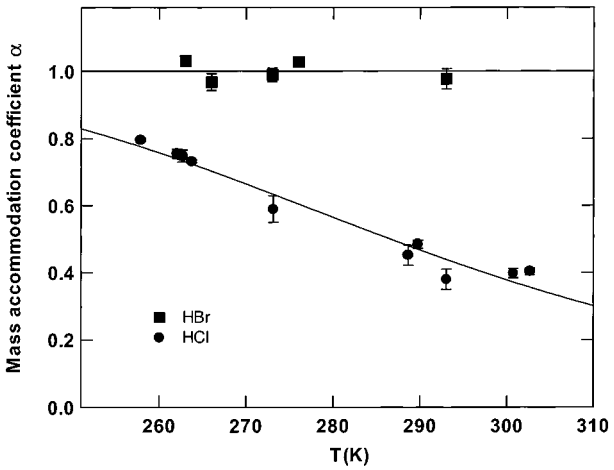

Figure 5. Mass accommodation coefficient (α) for HCl (circles) and HBr (squares) on ethylene glycol as a function of temperature. Solid line for HCl is obtained via eq 8 with $\Delta H_{obs} = -6.4 \pm 0.5$ kcal/mol and $\Delta S_{obs} = -22.3 \pm 1.9$ cal/(mol K). Solid line for HBr is the best straight-line fit to the data.

eq 4. As is evident, our formulation of gas-phase diffusion provides a good fit to the experimental data. These gas-phase diffusion studies are in accord with previous experiments conducted with sulfuric acid and water droplets.[27,38]

In Figure 4 the asymptote at large *Kn*, designated as γ_0, is the uptake coefficient in the limit of "zero pressure", i.e., in the absence of gas phase diffusion limitation. As is evident from eq 3, for HCl, γ_0 is α, which in this case, at 273 K, is 0.59 ± 0.01. (The limits indicate precision.) Additional *Kn* plots yield α for HCl(g) on ethylene glycol as a function of temperature. For both HBr and DCl the asymptote in Figure 4 is $\gamma_0 = 1.01 \pm 0.01$, independent of temperature. For HBr, $\gamma_0 = \alpha = 1$. The parameter γ_0 as a function of temperature is plotted in Figure 5 for both HCl and HBr. For DCl, $\gamma_0 = [\alpha(1 - p_{ex}) + p_{ex}] = 1$. Since α for HCl on ethylene glycol is not equal to 1, we can assume that α for DCl on ethylene glycol is likewise not equal to 1. With $\alpha \neq 1$, $\gamma_0 = [\alpha(1 - p_{ex}) + p_{ex}] = 1$ implies that $p_{ex} = 1$.[39]

Following the same procedures, the uptake coefficient (γ_{meas}) was obtained for HCl(g) and HBr(g) on pure ethylene glycol

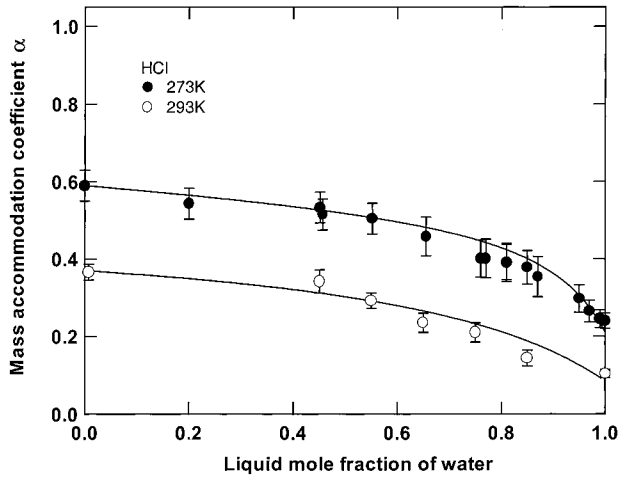

Figure 6. Mass accommodation coefficient α for HCl on ethylene glycol−water surfaces as a function of water mole fraction from 0 to 1 at 273 (filled symbols) and 293 K (open symbols). Solid lines are the calculations based on a model discussed in the text.

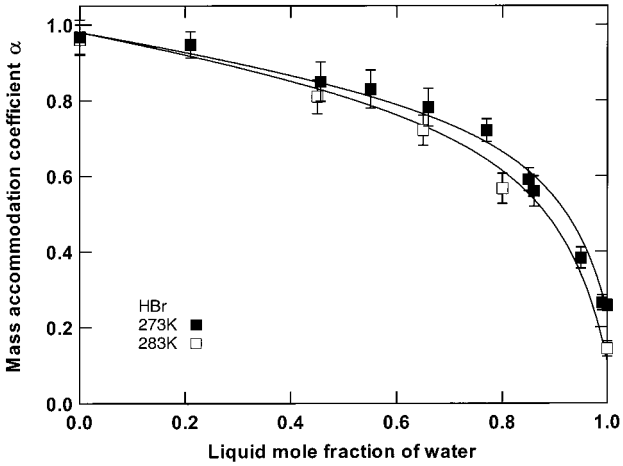

Figure 7. Mass accommodation coefficient α for HBr on ethylene glycol−water surfaces as a function of water mole fraction from 0 to 1 at 273 (filled symbols) and 283 K (open symbols). Solid lines are the calculations based on a model discussed in the text.

TABLE 1: Mass Accommodation Coefficient (α) for HCl on Pure Ethylene Glycol as a Function of Temperature

T (K)	258	262	263	264	273
α	0.80 ± 0.01	0.76 ± 0.01	0.75 ± 0.02	0.73 ± 0.01	0.59 ± 0.04
T (K)	289	290	293	301	303
α	0.45 ± 0.03	0.48 ± 0.01	0.38 ± 0.03	0.40 ± 0.02	0.40 ± 0.01

as a function of temperature and on ethylene glycol−water surfaces as a function of water mole fraction from 0 to 1. As was stated, detailed measurements with the solutions were performed at two temperatures: at 273 and 293 K for HCl and at 273 and 283 K for HBr. The water and ethylene glycol vapor pressures were set to be in equilibrium with the liquid droplet composition as stated earlier.

The mass accommodation coefficients (α) for HCl and HBr as a function of temperature, obtained from the uptake measurements, are shown in Figure 5. Values of α as a function of liquid mole fraction of water, are shown in Figures 6 and 7 for HCl and HBr, respectively. The solid lines in the figures are calculations based on models discussed in the following section. The data in Figures 5−7 are also presented in tabular form as Tables 1−6.

The mass accommodation coefficients for HCl on pure water obtained in this study are in agreement with previous measurements.[40,41] However, α for HBr on pure water measured in this study is about a factor of 2 higher than that obtained by Schweitzer et al.[41] The reason for this difference is at this point not evident. The precision of the measurements in this work is about ±2%. The accuracy is estimated to be about ±15%.

TABLE 2: Mass Accommodation Coefficient (α) for HBr on Pure Ethylene Glycol as a Function of Temperature

T (K)	263	266	273	276	293
α	1.03 ± 0.01	0.97 ± 0.02	0.99 ± 0.02	1.03 ± 0.01	0.98 ± 0.03

TABLE 3: Mass Accommodation Coefficient (α) for HCl on Ethylene Glycol−Water Surfaces as a Function of Water Liquid Mole Fraction X_{H_2O} at 273 K

X_{H_2O}	0	0.20	0.45	0.46
α	0.59 ± 0.04	0.54 ± 0.04	0.53 ± 0.04	0.52 ± 0.04
X_{H_2O}	0.55	0.66	0.76	0.77
α	0.50 ± 0.04	0.46 ± 0.05	0.40 ± 0.05	0.40 ± 0.05
X_{H_2O}	0.81	0.81	0.85	0.87
α	0.39 ± 0.05	0.39 ± 0.05	0.38 ± 0.04	0.35 ± 0.05
X_{H_2O}	0.95	0.97	0.99	1
α	0.30 ± 0.04	0.27 ± 0.03	0.25 ± 0.02	0.24 ± 0.02

TABLE 4: Mass Accommodation Coefficient (α) for HCl on Ethylene Glycol−Water Surfaces as a Function of Water Liquid Mole Fraction X_{H_2O} at 293 K

X_{H_2O}	0	0.45	0.55	0.65
α	0.37 ± 0.02	0.34 ± 0.03	0.29 ± 0.03	0.24 ± 0.03
X_{H_2O}	0.75	0.85	1	
α	0.21 ± 0.03	0.14 ± 0.02	0.10 ± 0.01	

TABLE 5: Mass Accommodation Coefficient (α) for HBr on Ethylene Glycol−Water Surfaces as a Function of Water Liquid Mole Fraction X_{H_2O} at 273 K

X_{H_2O}	0	0.21	0.46	0.55
α	0.97 ± 0.05	0.95 ± 0.04	0.85 ± 0.05	0.83 ± 0.05
X_{H_2O}	0.66	0.77	0.85	0.86
α	0.78 ± 0.05	0.72 ± 0.03	0.59 ± 0.03	0.56 ± 0.04
X_{H_2O}	0.95	0.99	1	
α	0.38 ± 0.03	0.27 ± 0.02	0.26 ± 0.02	

TABLE 6: Mass Accommodation Coefficient (α) for HBr on Ethylene Glycol−Water Surfaces as a Function of Water Liquid Mole Fraction X_{H_2O} at 283 K

X_{H_2O}	0	0.45	0.65	0.80	1
α	0.96 ± 0.04	0.81 ± 0.05	0.72 ± 0.04	0.57 ± 0.04	0.14 ± 0.02

Discussion

In this section uptake results on pure ethylene glycol are discussed first. Discussion of uptake measurements on the mixed ethylene glycol−water surfaces follow.

The thermal accommodation coefficient (S) for HCl on an ethylene glycol surface was not measured directly. However, the measured value of the isotope exchange probability of DCl on ethylene glycol, $p_{ex} = 1$, implies that every DCl (and therefore also HCl) molecule that strikes the surface interacts strongly with other surface molecules. This strong interaction is required to promote the ionic processes that control D/H isotope exchange.[34] Molecular interactions that can promote isotope exchange are expected to be also effective in thermalizing the species. Therefore, we suggest that $p_{ex} = 1$ indicates that the thermal accommodation coefficient S is likewise unity. A similar conclusion was reached in a recent study of $D_2O(g)$ uptake on liquid water.[42] A value of $S = 1$ is also consistent with molecular beam scattering studies, which show that, for molecules colliding at low energies with low vapor pressure

hydrogen-bonding liquids such as glycerol or sulfuric acid, the thermal accommodation coefficient is unity.[43,44]

As is shown in Figure 5, the mass accommodation coefficient for HCl on ethylene glycol increases from about 0.40 ± 0.01 at 303 K to 0.79 ± 0.01 at 258 K. Such a negative temperature dependence for α was observed in our previous uptake studies conducted with 30 or so hydrophilic gas-phase species including alcohols, hydrogen peroxide, and acetone on aqueous surfaces. As shown in the figure, the value of α for HBr is near unity independent of temperature in the range studied. These results are consistent with the following formulation of mass accommodation that was also applied to mass accommodation of gas molecules on water.

With $S = 1$, following eq 5, the mass accommodation coefficient can be expressed as[45]

$$\frac{\alpha}{1-\alpha} = \frac{k_{sol}}{k_{des}} = \frac{\exp(-\Delta G_{sol}/RT)}{\exp(-\Delta G_{des}/RT)} = \exp\left(\frac{-\Delta G_{obs}}{RT}\right) \quad (8)$$

The parameter $\Delta G_{obs} = \Delta H_{obs} - T\Delta S_{obs}$ is the Gibbs energy of the transition state between molecules in the gas phase and molecules solvated in the liquid phase. The solid line through the HCl experimental α-values in Figure 5 is the best fit to the data of eq 8, with $\Delta H_{obs} = -6.4 \pm 0.5$ kcal/mol and $\Delta S_{obs} = -22.3 \pm 1.9$ cal/(mol K).

Within the experimental accuracy, the mass accommodation coefficient of HBr on ethylene glycol is 1. In fact, the formulation in eq 8 precludes the value of α to be exactly 1. ($\alpha = 1$ implies that $k_{sol}/k_{des} = \infty$.) Therefore, in the context of eq 8, the α-value for HBr is understood to be close to, but not equal to, 1. For example, a value of $\alpha > 0.99$ implies $k_{sol}/k_{des} > 99$ and $-\Delta G_{obs}/RT > 4.6$. Since the mass accommodation coefficient of HBr is independent of temperature within the precision of the measurements, individual values for ΔH_{obs} and ΔS_{obs} cannot be determined in this case.

The larger value of α for HBr on ethylene glycol indicates (via eq 8) that the ratio of k_{sol}/k_{des} is larger for HBr than for HCl. That is, HBr interacts more strongly with the hydrophilic ethylene glycol surface than does HCl. This is consistent with the molecular beam scattering studies of Morris et al.,[46] which showed that on a 70 wt % D_2SO_4 surface thermalized HBr molecules undergo H−D exchange more readily than HCl molecules.

The functional form for ΔG_{obs} depends on the theoretical formulation of the uptake process. Therefore, the parameter ΔG_{obs} serves as a bridge between experiment and theory. Uptake studies on water surfaces led to the formulation of an uptake model in which the gas−liquid surface is envisioned as dynamic region where small clusters or aggregates of liquid molecules are expected to be continually forming, falling apart, and reforming. The driving force, as described by nucleation theory, is such that clusters smaller than a critical size fall apart, whereas clusters larger than the critical size serve as centers for further aggregation and grow in size until they merge into the adjacent bulk liquid. In this model, gas uptake proceeds via such growth of critical clusters. The incoming gas molecule upon striking the surface becomes a loosely bound surface species that participates in the surface nucleation process. If such a molecule becomes part of a critical size cluster, it will invariably be incorporated into the bulk liquid via cluster growth.[45,44] The present results suggest that this model may also apply to the ethylene glycol surface.

We note from the $X_{H_2O} = 0$ and 1 end points in Figures 6 and 7 that the mass accommodation coefficients for HCl and HBr(g) on pure ethylene glycol are higher than on pure water. At this point we do not have a clear compelling explanation for this observation. A notable difference between the two liquids is the larger dipole moment of ethylene glycol. The dipole moments for water and ethylene glycol are 1.8 and 2.2 D, respectively. (The values vary by about 5% depending on the medium within which the parameter is measured.) The larger dipole moment of ethylene glycol may result in the stronger binding of HCl and HBr to the ethylene glycol liquid surface than to water. This in turn may decrease k_{des} and perhaps also increase the nucleation rate (k_{sol}) resulting in the larger value of α. (See eq 8.)

The mass accommodation coefficients for HCl or HBr(g) on mixed ethylene glycol−water surfaces follow, in a general way, the expected pattern. At 0 mole fraction of water ($X_{H_2O} = 0$) the α-values are those measured on pure ethylene glycol, decreasing to the measured values of α on pure water at $X_{H_2O} = 1$. In between, α seems to follow a composition-weighted sum of the individual α-values for ethylene glycol and water. Since the decrease between the two end points is not a straight line, the weighting factor is not simply the liquid mole fraction of the mixture. This is not surprising since mass accommodation is a surface, rather than a bulk-phase phenomenon.

A reasonably good fit to the experimentally measured α-values for ethylene glycol−water solutions is obtained with the nucleation cluster model for mass accommodation. Here the uptake parameter ΔG_{obs} is calculated, as described in refs 44 and 45, for clusters composed of ethylene glycol and water molecules appropriately weighted in proportion to the surface coverage.

The nucleation model provides a basic understanding of the uptake process. However, the model includes variable parameters that limit its predictive usefulness. We therefore seek a simpler approach to modeling the results obtained in these experiments. As was stated, mass accommodation is a surface phenomenon. Therefore, it might be reasonable to suggest that the mass accommodation coefficient on the ethylene glycol−water solution is weighted by the fractional surface coverage $X(s)_{H_2O}$ as

$$\alpha = \alpha_{H_2O} X(s)_{H_2O} + \alpha_{EG}(1 - X(s)_{H_2O}) \quad (9)$$

where α is the mass accommodation coefficient of HCl(g) or HBr(g) on the ethylene glycol−water solution and the subscripted α's are the mass accommodation coefficients on pure water and pure ethylene glycol.[47]

The question is how to calculate $X(s)_{H_2O}$. Unfortunately, there is no well-established method for determining fractional surface coverage given the bulk-phase composition of a solution. We have calculated surface coverage in three ways. All are intuitively reasonable, but none is firmly rooted in equilibrium thermodynamics.

These methods are all based on relationships involving surface tension. Further, the formulations assume that a surface layer determines the surface tension. The surface tensions for pure water and ethylene glycol as a function of temperature are well established.[48,49] At 273 K they are $\sigma_{H_2O} = 75.64$ mN/m and $\sigma_{EG} = 50.33$ mN/m. The surface tension of ethylene glycol−water solutions as a function of water liquid mole fraction has been measured in the temperature range 283−323 K. The experimental results were generalized to yield an empirical formula for the surface tension of the solution as a function of temperature.[49]

In the first method, which has been used in several previous studies (see, for example, Butler and Wightman[50] and Guggen-

TABLE 7: Fractional Surface Coverage of Water, $X(s)_{H_2O}$, as a Function of Bulk Phase Mole Fraction X_{H_2O}: (i) Computed via Eqs 11 and 12; (ii) Computed via Eq 15; and (iii) Computed via Eq 16

X_{H_2O}	0	0.1	0.2	0.3	0.4	0.5	0.6	0.7	0.8	0.9	1
$X(s)_{H_2O}$ (i)	0	0.030	0.062	0.094	0.13	0.19	0.25	0.32	0.40	0.51	1
$X(s)_{H_2O}$ (ii)	0	0.029	0.055	0.082	0.12	0.16	0.21	0.27	0.37	0.54	1
$X(s)_{H_2O}$ (iii)	0	0.035	0.072	0.11	0.15	0.20	0.26	0.33	0.43	0.59	1

heim and Adam[51]) fractional surface coverage is computed via the surface excess. For a binary system, the surface excess of component 2 is given by the Gibbs equation:

$$\Gamma_2^1 = -\frac{a}{RT}\left(\frac{\partial\sigma}{\partial a}\right)_T \tag{10}$$

Here a is the activity of component 2, which in the case of the near-ideal ethylene glycol−water solution, can be replaced by the concentration. Given the measured value of the surface tension (σ) as a function of concentration, Γ_2 is computed using eq 10. The surface excess is a relative quantity and does not by itself provide a value for the surface coverage. Other relationships need to be invoked to obtain this quantity. It follows from the definition of surface excess[50,51] that

$$\Gamma_2 = N_2^{\,s} - N_1^{\,s}X_2/X_1 \tag{11}$$

Here N_1^s and N_2^s are the surface number densities of the species (no./cm^2) and X_1 and X_2 are the bulk-phase mole fractions. The other required equation can be formed in terms of the surface areas of A_1 and A_2 of the two molecules. That is

$$A_1N_1^{\,s} + A_2N_2^{\,s} = 1 \tag{12}$$

Here $A_1N_1^s$ and $A_2N_2^s$ are of course the fractional surface coverages, $X(s)_1$ and $X(s)_2$, of the species. Implicit in the formulation of eq 12 is the assumption that the surface excess is associated with a monolayer.

To calculate the surface coverage via eqs 11 and 12, one must first obtain values for the molecular surface areas A_1 and A_2. We obtained these parameters from the densities of the two species, assuming that the molecules in the liquid occupy space as if they were close-packed spheres. This approach yields areas 1.16×10^{-15} cm^{-2} and 2.47×10^{-15} cm^{-2} for water and ethylene glycol, respectively.

The second method, suitable for ideal mixtures, is based on a formulation presented by Defay and Prigogine:[52]

$$\sigma = \sigma_1 + \frac{kT}{A_1}\ln\frac{X_1^{\,s}}{X_1} = \sigma_2 + \frac{kT}{A_2}\ln\frac{X_2^{\,s}}{X_2} \tag{13}$$

Here σ_1 and σ_2 are the surface tensions of the pure liquids (in this case water and ethylene glycol), X_1^s and X_2^s are surface mole fractions, k is the Boltzmann constant, and A_1 and A_2 are as defined in eq 12. Equation 13 is solved iteratively for X_1^s and X_2^s. We note that X_1^s and X_2^s obtained via eq 13 must be distinguished from fractional surface coverages $X(s)_1$ and $X(s)_2$. The two are related by

$$X_1^{\,s} = \frac{N_1^{\,s}}{N_1^{\,s} + N_2^{\,s}} \tag{14}$$

yielding via eq 12

$$X(s)_1 = \frac{A_1X_1^{\,s}}{A_2 - A_2X_1^{\,s} + A_1X_1^{\,s}} \tag{15}$$

We propose here yet another, new, simpler method for calculating fractional surface coverage based on the assumption that the surface tension (σ) of the solution is simply given by

$$\sigma = \sigma_1X(s)_1 + \sigma_2(1 - X(s)_1) \tag{16}$$

Since σ as a function of bulk-phase water−ethylene glycol mole fraction is known, this formulation yields $X(s)_{H_2O}$ directly.

The fractional surface coverages of water ($X(s)_{H_2O}$) at 273 K, as a function of bulk-phase mole fraction of water, computed via the three methods, are shown in Table 7. As is evident, the $X(s)_{H_2O}$ values obtained via the three approaches agree, in most cases, to within about 15%. Further, as expected, the species with the lower surface tension (ethylene glycol) dominates the surface. The solid lines in Figures 6 and 7 are plots of eq 9 with the fractional surface coverage obtained from eq 16, which provides a somewhat better fit to the experimental data. This study suggests that surface tension may provide a reliable avenue for estimating other parameters associated with the surfaces of solutions composed of hydrophilic organic liquids and water.

Acknowledgment. Funding for this work was provided by the National Science Foundation Grants ATM-99-05551 and CH-0089147, by the Department of Energy Grant DE-FG02-98ER62581, and by the US−Israel Binational Science Foundation Grant 1999134. 53. We thank Prof. G. M. Nathanson for helpful comments and suggestions.

References and Notes

(1) Rosenfeld, D. *Science* **2000**, *287*, 1793.
(2) Kalberer, M.; Ammann, M.; Arens, F.; Gaggeler, H. W.; Baltensperger, U. *J. Geophys. Res.* **1999**, *104*, 13825.
(3) Longfellow, C. A.; Ravishankara, A. R.; Hanson, D. R. *J. Geophys. Res.* **1999**, *104*, 13833.
(4) Jacob, D. J. *Atmos. Environ.* **2000**, *34*, 2131.
(5) Gray, H. A.; Cass, G. R.; Huntzicker, J. J.; Heyerdahl, E. K.; Rau, J. A. *Environ. Sci. Technol.* **1986**, *20*, 580.
(6) Larson, S. M.; Cass, G. R.; Gray, H. A. *Aerosol Sci. Technol.* **1989**, *10*, 118.
(7) Novakov, T.; Penner, J. E. *Nature* **1993**, *365*, 823.
(8) Pandis, S. N.; Wexler, A. S.; Seinfeld, J. H. *J. Phys. Chem.* **1995**, *99*, 9646.
(9) Cruz, C. N.; Pandis, S. N. *Atmos. Environ.* **1997**, *31*, 2205.
(10) Novakov, T.; Corrigan, C. E.; Penner, J. E.; Chuang, C. C.; Rosario, O.; Bracero, O. L. M. *J. Geophys. Res.* **1997**, *102*, 21307.
(11) Murphy, D. M.; Thomson, D. S.; Mahoney, M. J. *Science* **1998**, *282*, 1664.
(12) Facchini, M. C.; Mircea, M.; Fuzzi, S.; Charlson, R. J. *Nature* **1999**, *401*, 257.
(13) Moise, T.; Rudich, Y. *J. Geophys. Res.-Atmos.* **2000**, *105*, 14667.
(14) Saxena, P.; Hildemann, L. M. *J. Phys. Chem.* **1995**, *24*, 57.
(15) Andrews, E.; Kreidenweis, S. M.; Penner, J. E.; Larson, S. M *J. Geophys. Res.* **1997**, *102*, 21997.
(16) Kavouras, L. G.; Milhalopoulos, N.; Stephanon, E. G. *Nature* **1998**, *395*, 683.
(17) Limbeck, A.; Puxbaum, H. *Atmos. Environ.* **1999**, *33*, 1847.
(18) Griffin, R. J.; Cocker, D. R.; Seinfeld, J. H.; Dabdub, D. *Geophys. Res. Lett.* **1999**, *26*, 2721.
(19) Odum, J. R.; Jungkamp, T. P. W.; Griffin, R. J.; Flagan, R. C.; Seinfeld, J. H. *Science* **1997**, *276*, 96.
(20) Odum, J. R.; Jungkamp, T. P. W.; Griffin, R. J.; Forstner, H. J. L.; Flagan, R. C.; Seinfeld, J. H. *Sci. Technol.* **1997**, *31*, 1890.
(21) Hoffmann, T.; Odum, J. R.; Bowman, F.; Collins, D.; Klockow, D.; Flagan, R. C.; Seinfeld, J. H. *J. Atmos. Chem.* **1997**, *26*, 189.
(22) Blando, J. D.; Porcja, R. J.; Li, T. H.; Bowman, D.; Lioy, P. J.; Turpin, B. J. *Environ. Sci. Technol.* **1998**, *32*, 604.
(23) Andreae, M. O.; Crutzen, P. J. *Science* **1997**, *276*, 1052.

(24) Jacobson, M. C.; Hansson, H.-C.; Noone, K. J.; Charlson, R. J. *Rev. Geophys*. **2000**, *38*, 267.

(25) Turpin B. J.; Saxena, P.; Andrews, E. *Atmos. Environ*. **2000**, *34*, 2983.

(26) Shi, Q.; Davidovits, P.; Jayne, J. T.; Worsnop, D. R.; Kolb, C. E. *J. Phys. Chem*. A **1999**, *103*, 8812.

(27) Worsnop, D. R.; Shi, Q.; Jayne, J. T.; Kolb, C. E.; Swartz, E.; Davidovits, P. *J. Aerosol Sci*. **2001**, *32*, 877.

(28) Fuchs, N. A.; Sutugin, A. G. *Highly Dispersed Aerosols*; Ann Arbor Science Publishers: Ann Arbor, MI, 1970.

(29) Widmann, J. F.; Davis, E. J. *J. Aerosol Sci*. **1997**, *28*, 87.

(30) Seinfeld, J. H.; Pandis, S. N. *Atmospheric Chemistry and Physics*; John Wiley & Sons: 1998; p 602.

(31) Hanson, D. R.; Ravishankara, A. R.; Lovejoy, E. R. *J. Geophys. Res.* **1996**, *101*, 9063.

(32) Worsnop, D. R.; Zahniser, M. S.; Kolb, C. E.; Gardner, J. A.; Watson, L. R.; Van Doren, J. M.; Jayne, J. T.; Davidovits, P. *J. Phys. Chem.* **1989**, *93*, 1159.

(33) Jayne, J. T.; Duan, S. X.; Davidovits, P.; Worsnop, D. R.; Zahniser, M. S.; Kolb, C. E. *J. Phys. Chem*. **1991**, *95*, 6329.

(34) Shi, Q.; Li, Y. Q.; Davidovits, P.; Jayne, J. T.; Worsnop, D. R.; Mozurkewich, M.; Kolb, C. E. *J. Phys. Chem. B* **1999**, *103*, 2417.

(35) Trimble, H. M.; Potts, W. *Ind. Eng. Chem*. **1935**, *27*, 66.

(36) Gmehling, J.; Onken, U. *Vapor-liquid equilibrium data collection, DeChema Chemistry Data Series*; Scholium Publ. Inc.: Flushing, NY, 1977.

(37) Nath, A.; Bender, E. *J. Chem. Eng. Data* **1983**, *28*, 370.

(38) Swartz, E.; Shi, Q.; Davidovits, P.; Jayne, J. T.; Worsnop, D. R.; Kolb, C. E. *J. Phys. Chem*. *A* **1999**, *103*, 8824.

(39) In an independent set of control experiments, we measured the uptake of DCl on 1-methylnaphthalene ($C_{11}H_{10}$). The uptake and therefore also the isotope exchange coefficient was below our detection limit, that is, $\gamma_{meas} < 5 \times 10^{-4}$.

(40) Van Doren, J. M.; Watson, L. R.; Davidovits, P.; Worsnop, D. R.; Zahniser, M. S.; Kolb, C. E. *J. Phys. Chem.* **1990**, *94*, 3265.

(41) Schweitzer, F.; Mirabel, P.; George, C. *J. Phys. Chem. A* **2000**, *104*, 72.

(42) Li, Y. Q.; Davidovits, P.; Shi, Q.; Jayne, J. T.; Kolb, C. E.; Worsnop, D. R. Submitted for publication.

(43) Saecker, M. E.; Nathanson, G. M. *J. Phys. Chem*. **1993**, *99*, 7056.

(44) Nathanson, G. M.; Davidovits, P.; Worsnop, D. R.; Kolb, C. E. *J. Phys. Chem*. **1996**, *100*, 13007.

(45) Davidovits, P.; Jayne, J. T.; Duan, S. X.; Worsnop, D. R.; Zahniser, M. S.; Kolb, C. E. *J. Phys. Chem*. **1991**, *95*, 6337.

(46) Morris, J. R.; Behr, P.; Antman, M. D.; Ringeisen, B. R.; Splan, J.; Nathanson, G. M. *J. Phys. Chem*. *A* **2000**, *104*, 6738.

(47) Equation 9 is to be regarded as an empirical formulation. It does not include explicitly a mixed $X(s)_{H_2O}$ and $X(s)_{EG}$ term which would take into account uptake via critical clusters containing both water and ethylene glycol molecules. It is not clear how to include the mixed term in the simple formulation of eq 9. We have tried several approaches. In the simplest approach we assume that fraction "*a*" of incoming gas-phase species is governed by the mixed process with an average α_{mix} given by $\alpha_{mix} = \alpha_1 X(s)_1 + \alpha_2 X(s)_2$. A possible expression for the overall α may then be:

$$\alpha = (1 - a)\alpha_1 X(s)_1 + (1 - a)\alpha_2 X(s)_2 + a(\alpha_1 X(s)_1 + \alpha_2 X(s)_2)$$

This is eq 9. More complex expressions involving powers of $X(s)$ to account for the probabilistic nature of the process have also been tried. However, they do not provide a better fit to the data nor can their validity be more convincingly demonstrated.

(48) *Handbook of Chemistry and Physics*, 73rd ed.; CRC Press: Boca Raton, FL, 1992−1993; pp 6−10.

(49) Tsierkezos, N. G.; Molinou, I. E. *J. Chem. Eng. Data* **1998**, *43*, 989.

(50) Butler, J. A. V.; Wightman, A. *J. Chem. Soc*. **1932**, 2089.

(51) Guggenheim, E. A.; Adam, N. K. *Proc. R. Soc., London* **1933**, *A139*, 218.

(52) Defay, R.; Prigogine, I. *Surface Tension and Adsorption*; John Wiley & Sons: New York, 1966; p 167.